Neurobiology of Disease 43 (2011) 678–689

Contents lists available at ScienceDirect

Neurobiology of Disease

journal homepage: www.elsevier.com/locate/ynbdi

Cerebral cortex demyelination and oligodendrocyte precursor response to experimental autoimmune encephalomyelitis

Francesco Girolamo [a,*], Giovanni Ferrara [b], Maurizio Strippoli [a], Marco Rizzi [a], Mariella Errede [a], Maria Trojano [c], Roberto Perris [d,e], Luisa Roncali [a], Maria Svelto [f], Tiziana Mennini [b], Daniela Virgintino [a]

[a] Department of Human Anatomy and Histology, University of Bari School of Medicine, Piazza Giulio Cesare, 11, 70124, Bari, Italy
[b] Department of Biochemistry and Molecular Pharmacology, Mario Negri Institute for Pharmacological Research, via La Masa, 19, 20156, Milano, Italy
[c] Department of Neurological and Psychiatric Sciences, University of Bari School of Medicine, Piazza Giulio Cesare, 11, 70124, Bari, Italy
[d] Division for Experimental Oncology 2, The National Cancer Institute Aviano, CRO-IRCCS, Via F. Gallini, 2, 33081, Aviano, Italy
[e] Department of Genetics, Microbiology and Anthropology, University of Parma, Via G.P. Usberti, 11/A, 43100, Parma, Italy
[f] Department of General and Environmental Physiology and Centre of Excellence in Comparative Genomics (CEGBA), University of Bari, via Amendola, 165/A, 70124, Bari, Italy

ARTICLE INFO

Article history:
Received 28 February 2011
Revised 6 May 2011
Accepted 28 May 2011
Available online 6 June 2011

Keywords:
Experimental autoimmune encephalomyelitis
Cerebral cortex demyelination
Oligodendrocyte lineage
OPCs/polydendrocytes
Multiple sclerosis
Immunofluorescence confocal microscopy

ABSTRACT

Experimentally induced autoimmune encephalomyelitis (EAE) in mice provides an animal model that shares many features with human demyelinating diseases such as multiple sclerosis (MS). To what extent the cerebral cortex is affected by the process of demyelination and how the corollary response of the oligodendrocyte lineage is explicated are still not completely known aspects of EAE. By performing a detailed *in situ* analysis of expression of myelin and oligodendrocyte markers we have identified areas of subpial demyelination in the cerebral cortex of animals with conventionally induced EAE conditions. On EAE-affected cerebral cortices, the distribution and relative abundance of cells of the oligodendrocyte lineage were assessed and compared with control mouse brains. The analysis demonstrated that $A2B5^+$ glial restricted progenitors (GRPs) and $NG2^+$/PDGFR-α^+ oligodendrocyte precursor cells (OPCs) were increased in number during "early" disease, 20 days post MOG immunization, whereas in the "late" disease, 39 days post-immunization, they were strongly diminished, and there was an accompanying reduction in $NG2^+/O4^+$ pre-oligodendrocytes and GST-π mature oligodendrocytes. These results, together with the observed steady-state amount of $NG2^-/O4^+$ pre-myelinating oligodendrocytes, suggested that oligodendroglial precursors attempted to compensate for the progressive loss of myelin, although these cells appeared to fail to complete the last step of their differentiation program. Our findings confirm that this chronic model of EAE reproduces the features of neocortex pathology in progressive MS and suggest that, despite the proliferative response of the oligodendroglial precursors, the failure to accomplish final differentiation may be a key contributing factor to the impaired remyelination that characterizes these demyelinating conditions.

Introduction

Experimental autoimmune encephalomyelitis (EAE) is a widely used animal model characterized by inflammatory demyelination of the central nervous system (CNS), as occurs in the human disease multiple sclerosis (MS). Disease heterogeneity in terms of clinical course and neuropathology is characteristic of MS (Lucchinetti et al., 2000) and is also a feature of EAE. In fact, in the latter, depending upon the species, strain, immunization protocol and dosage of the immunogen, relapsing–remitting or chronic models can be reproduced (Berard et al., 2010; Gold et al., 2006). In patients with progressive MS the brain is globally affected, as a consequence of the persistent and diffuse inflammatory process, showing diffuse demyelination, axonal loss and microglial activation in normal appearing WM as well as in deep and cortical grey matter (GM) (Bø et al., 2003; Bø, 2009; Kidd et al., 1999; Kutzelnigg et al., 2005; Peterson et al., 2001; Rudick and Trapp, 2009). Although only a marginal correlation between focal WM lesions and cortical

Abbreviations: CNPase, 2′,3′-Cyclic Nucleotide 3′-Phosphodiesterase; dpi, days post MOG immunization; EAE, Experimental Autoimmune Encephalomyelitis; GFAP, Glial Fibrillary Acidic Protein; GRP, glial restricted progenitor; GST-π, glutathione S-transferase isoform-π; MBP, Myelin Basic Protein; MOG, Myelin Oligodendrocyte Glycoprotein; MS, Multiple Sclerosis; NeuN, Neuronal Nuclei; NF, Neurofilament; NG2, Nerve-glial antigen 2; OPC, oligodendrocyte precursor cell; PCNA, proliferative cell nuclear antigen; PDGFR-α, platelet derived growth factor receptor-α; PLP, Proteolipid Protein.

* Corresponding author. Fax: +39 080 5478310.
E-mail addresses: f.girolamo@histology.uniba.it (F. Girolamo), giovanni.ferrara@marionegri.it (G. Ferrara), mauriziostrippoli@libero.it (M. Strippoli), marcorizzi.mr@libero.it (M. Rizzi), m.errede@histology.uniba.it (M. Errede), mtrojano@neurol.uniba.it (M. Trojano), rperris@cro.it (R. Perris), roncali@histology.uniba.it (L. Roncali), svelto@biologia.uniba.it (M. Svelto), tiziana.mennini@marionegri.it (T. Mennini), virgintino@histology.uniba.it (D. Virgintino).

Available online on ScienceDirect (www.sciencedirect.com).

0969-9961/$ – see front matter © 2011 Elsevier Inc. All rights reserved.
doi:10.1016/j.nbd.2011.05.021

pathology has been described, demyelination within cortical GM areas may contribute to disease progression and also play a role in the emergence of cognitive deficits (Chen et al., 2004; De Stefano et al., 2003; Geurts et al., 2009; Kutzelnigg et al., 2005; Lazeron et al., 2000; Stadelmann et al., 2008). Conventional EAE mouse models, including MOG-induced EAE, have been most commonly adopted to focus on spinal cord inflammation/demyelination (Gold et al., 2006), while neocortex demyelination has been primarily described in specifically designed experimental models (Pomeroy et al., 2005; Merkler et al., 2006; Storch et al., 2006). Data on cortical lesions were reported by Rasmussen et al. (2007) in relapsing–remitting rodent EAE induced by PLP and only very recently, forebrain demyelination has been demonstrated in chronic EAE, induced by MOG in C57BL/6 mice, that mimics primary and secondary progressive MS (Mangiardi et al., 2011).

Concurrently with destructive events, regenerative processes take place in MS and EAE demyelinated lesions of WM, including attempts by nervous tissue to remyelinate the damaged areas (Albert et al., 2007; Blakemore, 1974; Bunge et al., 1961; Franklin and ffrench-Constant, 2008; Patani et al., 2007; Prineas et al., 1993). The heterogeneity observed in the degree of remyelination in samples collected from autopsies and biopsies could be related to patients' age and MS clinical subtypes (Frohman et al., 2006; Lassmann et al., 1997; Goldschmidt et al., 2009; Patrikios et al., 2006). It has been demonstrated that some chronic MS lesions contain immature oligodendrocytes, which can be involved in the phenomenon of remyelination (Chang et al., 2000, 2002; Wolswijk, 1998, 2002), but a comprehensive analysis of the sequential maturation stages of oligodendrocyte lineage during chronic evolution of the disease is still lacking.

In the perinatal period of normal brain development, oligodendrocytes arise from precursors that differentiate through a series of stages identified by specific markers: glial restricted progenitors (GRPs) recognized by the phenotype marker A2B5 which corresponds to a specific group of gangliosides (Cameron and Rakic, 1991; Kundu et al., 1983; Liu et al., 2002; Steiner et al., 2007; Strathmann et al., 2007), oligodendrocyte precursor cells (OPCs) identified by NG2 (nerve-glial antigen 2) chondroitin sulphate proteoglycan and by PDGFR-α (platelet derived growth factor receptor-α), molecules both involved in cell proliferation and migration (He et al., 2009; Heldin and Westermark, 1999; Chekenya et al., 2008; Kucharova and Stallcup, 2010; Makagiansar et al., 2007), pre-oligodendrocytes also expressing NG2 and identified by the phenotype marker O4, which recognizes specific glycolipids and cholesterol (Bansal et al., 1989; Baumann and Pham-Dihn, 2001; Cai et al., 2006; Guardia Clausi et al., 2010; Probstmeier et al., 1999; Sommer and Schachner, 1981), myelinating oligodendrocytes that express myelin-associated proteins, MBP and MOG, and specific enzymes, CNPase and GST-π (Baumann and Pham-Dihn, 2001; Quarles, 1997; Tansey and Cammer, 1991). In the adult CNS, NG2-expressing cells, OPCs/polydendrocytes and pre-oligodendrocytes are still present. Polydendrocytes are morphologically and antigenically indistinguishable from OPCs but in normal conditions they represent a non-proliferating, stable cell population (Butt et al., 2005; Fruttiger et al., 1999; Goldman, 2005; Levine et al., 1993; Nishiyama et al., 1996, 2009).

Although several studies have described the presence of cells of the oligodendrocyte lineage in EAE demyelinating lesions of the spinal cord, relatively little is known about the situation in the cerebral cortex (Di Bello et al., 1999; Gensert and Goldman, 1997; Keirstead et al., 1998; Papadopoulos et al., 2010; Polito and Reynolds, 2005; Reynolds et al., 2002). Considering that the origin, identity and degree of maturation of the cells that may play an effective role during the remyelination process remain of primary interest, also in view of observations made on human MS lesions, in this study we have analyzed the presence and distribution of oligodendrocyte lineage cells in the cerebral cortex of MOG-induced chronic EAE. The antigenic phenotype of oligodendroglia precursors and myelinating oligodendrocytes has been revealed by a broad panel of cell-specific markers during "early" and "late" stages of the disease with the aim of defining the mode, extent, and course of the oligodendrocyte response in relation to the neocortex demyelination events.

Materials and methods

EAE induction and clinical evaluation

Procedures involving animals and their care were conducted in conformity with the institutional guidelines in compliance with national (D.L. n. 116, G.U., suppl. 40, Feb. 18, 1992) and international laws and policies (EEC Council Directive 86/609, OJ L 358, 1, Dec.12, 1987; Guide for the Care and Use of Laboratory Animals, U.S. National Research Council, 1996). The protocols for the proposed investigation were reviewed and approved by the Animal Care and Use Committees (IACUC) of the "Mario Negri" Institute for Pharmacological Research. Chronic EAE was induced in C57BL/6 wild type female mice (6–8 weeks of age) obtained from Harlan (Bresso, MI, Italy) and maintained in specific pathogen-free conditions. EAE was induced by subcutaneous immunization with a total of 200 μg of $MOG_{35–55}$ in incomplete Freund's adjuvant (Sigma, St. Louis, MO, USA), supplemented with 8 mg/ml of Mycobacterium tuberculosis (strain H37RA; Difco, Detroit, MI, USA). The mice received 300 ng of pertussin toxin (Sigma) i.v. at the immunization time and 48 h later. Control C57BL/6 female mice received a subcutaneous injection of incomplete Freund's adjuvant without $MOG_{35–55}$. Weight and clinical score (*cs*) were recorded daily according to the standard EAE grading scale. The onset of EAE clinical signs was at 13–14 days post-immunization (dpi). On the total immunized mice (n = 16), a first group of mice was sacrificed during "early EAE" (n = 9; *cs* 1.5 to 3.5) at 20 dpi, while a second group was followed up to 39 dpi, defined as "late EAE" (n = 6; *cs* 2.0 to 3.0). Individual clinical scores were plotted *per* day, data were expressed as median ± SEM (Supplementary Fig. 1). For each experimental group, healthy controls (n = 5) were sacrificed at equivalent times.

Histology and Immunohistochemistry

Mice were anesthetized with chloral hydrate (3 μl/g, intraperitoneal injection) and transcardially perfused with 100 ml of fixative (2% paraformaldehyde plus 0.2% glutaraldehyde). After perfusion, each hemisphere was cut into 20-μm thick sagittal sections then immunostained for light microscopy or confocal laser microscopy, except for sections that were stained with toluidine blue for comparative microanatomy analysis. The following primary antibodies were utilized in single and multiple immunolabelings: anti-MBP (Myelin Basic Protein), anti-A2B5, anti-NG2 (nerve-glial antigen 2), anti-NeuN (Neuronal Nuclei), anti-O4, anti-PDGFR-α (platelet derived growth factor receptor-α), anti-CNPase (2′,3′-Cyclic Nucleotide 3′-Phosphodiesterase), anti-MOG (Myelin Oligodendrocyte Glycoprotein, anti-GST-π (glutathione S-transferase isoform-π), anti-GFAP (Glial Fibrillary Acidic Protein), anti-NF (70 kDa Neurofilament), anti-CD45, anti-PCNA (Proliferative Cell Nuclear Antigen). The initial analysis of both cerebral cortex and subcortical white matter myelination levels, in healthy and EAE-affected mice, was carried out by immunoenzymatic methods to reveal the myelin marker MBP. Subsequently, adjacent sections were immunolabeled for laser confocal analysis with a number of markers (Table 1), according to the protocols described in the Supplementary materials. Sections were examined under a Leica TCS SP5 confocal laser scanning microscope (Leica Microsystems, Mannheim, Germany).

Quantitative assessment

Brains from healthy (n = 5), "early EAE" (20 dpi; n = 5), and "late EAE" (39 dpi; n = 5) mice were utilized for computer-aided morphometric analysis. The levels of brain myelination, in cerebral cortex

Table 1
Primary antibodies and secondary antibodies combined in single and multiple immunolabelings[a].

Primary antibodies	Host Ig	Dilution	Producer company	Code number
Anti-MBP	rabbit IgG	1:100	Abcam	ab65988
A2B5	mouse IgM	1:600	Millipore	MAB312R
Anti-NG2	rabbit IgG	1:200	Millipore	AB5320
Biotinylated anti-NeuN	mouse IgG_1	1:100	Millipore	MAB377B
O4	mouse IgM	1:1000	Millipore	MAB345
Anti-PDGFR-α	rat $IgG_{2a\ kappa}$	1:70	Millipore	CBL1366
Anti-CNPase	mouse IgG_1	1:60	Sigma	C5922
Anti-MOG	goat IgG	1:300	R&D Systems	AF2439
Anti-GST-π	rabbit IgG	1:750	MBL Int. Corp.	312
Anti-GFAP	mouse IgG_1	1:150	V.B. Novocastra	NCL-GFAP-GA5
Anti-NF	mouse IgG_1	1:80	Dako	M0762
Anti-CD45	rat IgG_2	1:50	Novus Biologicals	NB110-93609
Anti-PCNA	mouse IgG	1:70	Santa Cruz	Sc-56
Secondary antibodies and streptavidin conjugates		Dilution	Producer company	Code number
1	Biotinylated goat-anti-rabbit	1:500	Vector	BA-1000
2	HRP-streptavidin	1 μg/ml	Vector	SA-5704
3	Biotinylated goat anti-mouse IgM	1:300	Invitrogen	D20693
4	Streptavidin-conjugated Alexa 488	1:300	Invitrogen	S-11223
5	Streptavidin-conjugated Alexa 555	1:300	Invitrogen	S-21381
6	Goat anti-rabbit Alexa 568	1:300	Invitrogen	A11011
7	Goat anti mouse IgG_1 Alexa 488	1:300	Invitrogen	A11001
8	Donkey anti goat Alexa 488	1:300	Invitrogen	A11055
9	Goat anti-rabbit Alexa 488	1:300	Invitrogen	A11070
10	Donkey anti goat Alexa 568	1:300	Invitrogen	A11057
11	Goat anti mouse IgG_1 Alexa 633	1:300	Invitrogen	A21126
12	Goat anti rat Alexa 555	1:400	Invitrogen	A21434

[a] Primary antibodies combinations in multiple immunolabelings: A2B5 combined with NG2 (revealed by 3, 4, 6 immunoreagents, ir) or NeuN (3, 4, 5 ir); NG2 combined with GFAP (6, 7 ir), O4 (3, 4, 6 ir), CNPase (6, 7 ir), MOG (6, 8 ir), PCNA (6, 7 ir), PDGFR-α (9, 12 ir); MBP combined with MOG and CNPase (9, 10, 11 ir); MBP combined with NF (6, 8 ir); MBP combined with CD45 (9, 12 ir).

supragranular/granular layers and in subgranular layers/subcortical WM, were analyzed on sections immunostained with MBP or MOG. In the same areas, the number of cell precursors identified by their own phenotype, $A2B5^+/NG2^-$ GRPs (glial restricted progenitors), $NG2^+/PDGFR\text{-}\alpha^+$ OPCs (oligodendrocyte precursor cells), $NG2^+/O4^+$ pre-oligodendrocytes, and $NG2^-/O4^+/CNPase^+/GST\text{-}\pi$ pre-myelinating/myelinating oligodendrocytes, was interactively assessed, normalized to the same volume (1 mm^3) and expressed as mean value ± SD. Proliferating $NG2^+/PCNA^+$ OPCs were also counted and the results are expressed as percentages of the total $NG2^+$ cell number. For each marker, immunoreactive tissue areas were also measured and the results are expressed as mean value ± SD. All data were statistically analyzed using Student *t*-test, one-way Anova and the Bonferroni post-test (GraphPad Prism, GraphPad Software, Inc., La Jolla, CA, USA). Results were considered significant at *p*-values of <0.05.

Results

Immunolocalization of cells of the oligodendrocyte lineage in cerebral cortex of healthy mice

The distribution and characteristics of the cells of the oligodendrocyte lineage were evaluated in healthy mice with the aid of specific markers. On sections double immunolabeled for A2B5 and NG2, a number of $A2B5^+/NG2^-$ glial restricted progenitors (GRPs) were recognized throughout all the cerebral cortex layers (Supplementary Figs. 2a–c) and in subcortical white matter (WM) (Supplementary Figs. 2d–f). GRPs showed a typical morphology characterized by a small cell body and few, short processes (Supplementary Figs. 2a, c, d, f), easily distinguishable from the $A2B5^+/NeuN^+$ nuclei of cortex neurons (Ledeen and Wu, 2008) frequently detected in the upper part of cortical layer II (Supplementary Figs. 2a, c, g–i). $A2B5^-/NG2^+$ precursors were revealed in the cortex and in subcortical WM areas (Supplementary Figs. 2a–f), where they represented a large population of immature oligodendrocytes. These $NG2^+$ oligodendroglial precursors were morphologically different from the $A2B5^+$ progenitors, showing numerous long, slender processes forming a rich network throughout the neuropil (Supplementary Figs. 2a–f). A small percentage of $NG2^+$ cells, also reactive for A2B5 (0.5 ± 1.8%), characterized by few processes and preferentially localized in the subcortical WM, was also revealed (Supplementary Figs. 2d–f) and regarded as "transitional" oligodendrocyte precursors that would eventually differentiate into $A2B5^-/NG2^+$ oligodendrocyte precursors. Double immunostainings carried out with anti-NG2 and anti-O4 antibodies allowed us to distinguish, in the whole $NG2^+$ cell population, the $NG2^+/O4^-$ oligodendrocyte precursor cells (OPCs) from the $NG2^+/O4^+$ pre-oligodendrocytes, as well as to reveal $NG2^-/O4^+$ pre-myelinating oligodendrocytes (Supplementary Figs. 3a–f, j–l). On these sections, O4 stained glycolipids were also present in the neuropil, in particular in the subgranular cortex layers and in WM, where they were revealed on myelinated fibers (Supplementary Figs. 3a, c, d, f). In cortex and WM, NG2/O4 immunolabeling disclosed a large population of $NG2^+/O4^+$ pre-oligodendrocytes, distinct from the typical $NG2^+/O4^-$ OPCs (Supplementary Figs. 3a–f). As demonstrated by morphometric analysis, in normal cerebral cortex pre-oligodendrocytes outnumbered the OPCs and accounted for 60.9 ± 18.1% of the total $NG2^+$ cells. On the other hand, in the WM of these control brains, the pre-oligodendrocytes only represented 31.8 ± 21.7% of the entire $NG2^+$ cell population (Supplementary Figs. 3a–f). To accurately evaluate the $NG2^+/O4^-$ OPC population, double immunolabelings were carried out with NG2 and the OPC-specific marker PDGFR-α (Supplementary Figs. 3g–i). The percentage of $PDGFR\text{-}\alpha^+$ OPCs accounted for 55.2 ± 20.6% of the total $NG2^+$ cell population in supragranular and granular layers and for 76.7 ± 11.6% of the entire $NG2^+$ cells in subgranular layers and WM. On these sections, PDGFR-α staining appeared more concentrated in the cell body and showed a punctuate pattern on processes (Supplementary Figs. 3g–i). The remaining population of $NG2^+/O4^+$ pre-oligodendrocytes was characterized by a large cell body and a longer, more extended branching than OPCs (Supplementary Figs. 3j, l). In the middle layers of the cortex and in the WM, several $NG2^-/O4^+$ cell bodies and fibers of

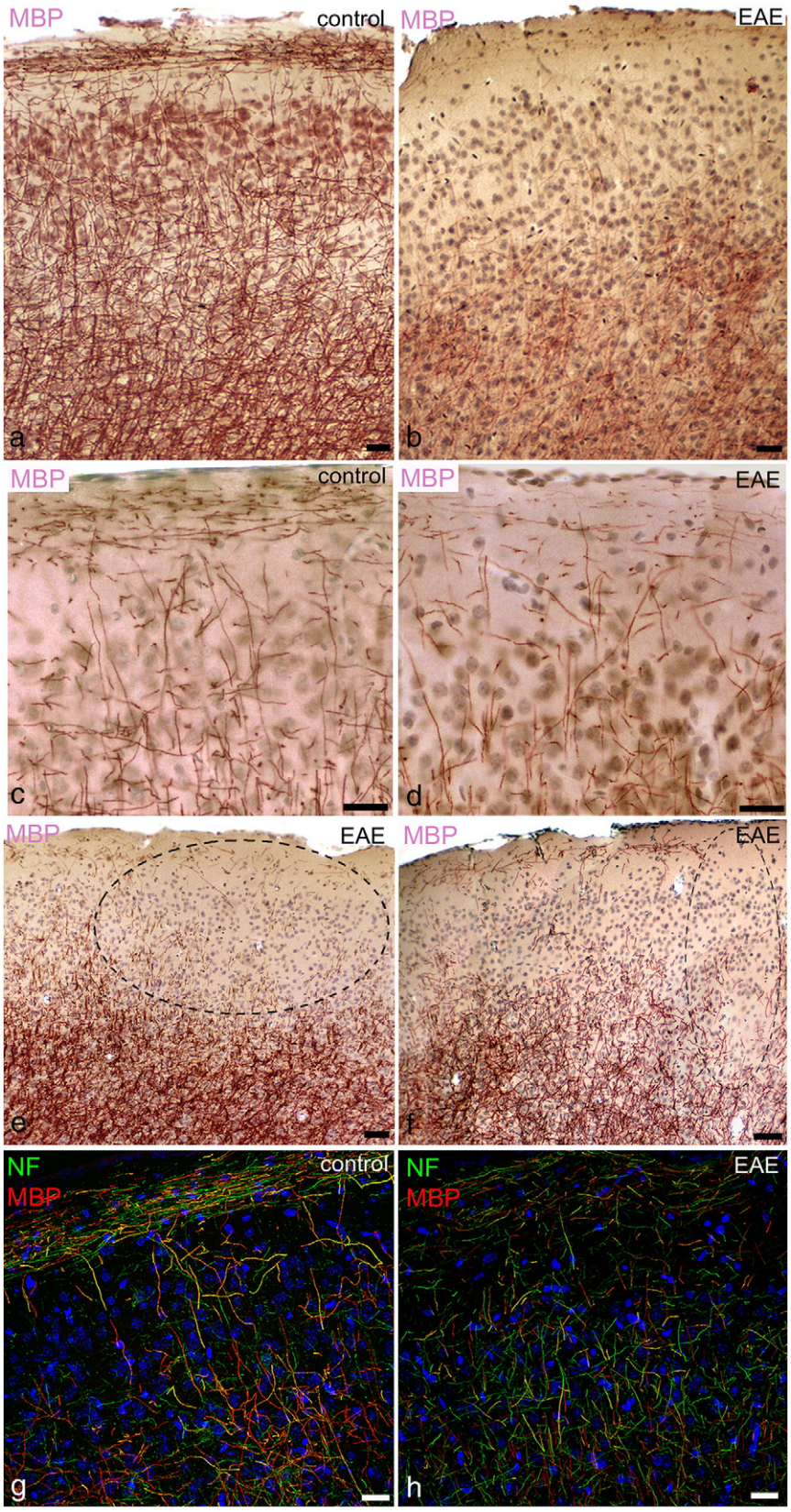

Fig. 1. Representative images of cerebral cortex immunolabeled for MBP and MBP/NF. (a–d) MBP staining in normal (a, c) and EAE (b, 39 dpi; d, 20 dpi) occipital cortex, showing a reduced MBP reactivity in EAE supragranular and granular layers; note in d, scarce, subpial fibers. (e, f) MBP staining in 39 dpi EAE mice showing frontal cortex demyelinated areas either limited to the outer layers (e, *dotted ellipse*) or extending throughout the cortex (f, *dotted ellipse*). (g, h) MBP^+/NF^+ nerve fibers in layers I and II of normal frontal cortex (g) compared to "naked" axons (h, *green*) in the cortex of 39 dpi EAE mice. Scale bars: 30 μm. (For interpretation of the references to colour in this figure legend, the reader is referred to the web version of this article.)

pre-myelinating oligodendrocytes were also evident (Supplementary Figs. 3c, f, l). Triple immunostainings were carried out with antibodies to CNPase, MBP and MOG to disclose mature, myelinating oligodendrocytes and myelinated nerve fibers. As expected, CNPase$^+$/MBP$^+$/MOG$^+$ oligodendrocytes and myelinated fibers were present in all the cortical layers as well as in the WM (Supplementary Figs. 4 a–d); in particular, CNPase staining also identified oligodendrocyte cell bodies (Supplementary Figs. 4 e–h), whereas MBP and MOG specifically tagged the myelinated fibers (Supplementary Figs. 4 f–h). In addition to these general myelin markers, and to better evaluate the amount of mature oligodendrocytes throughout the cortex and WM, single labelings were also carried out with the oligodendrocyte-specific enzyme GST-π, that specifically marks the cell body (Supplementary Figs. 5 a–c). Overall, the largest population of oligodendrocyte precursors described above appeared to be composed of NG2$^+$ oligodendroglial cells, one portion of which exhibited NG2$^+$/PDGFR-α$^+$/O4$^-$ OPC phenotype and the other one the more differentiated NG2$^+$/O4$^+$ pre-oligodendrocyte phenotype.

To highlight the relationship between the NG2$^+$ oligodendroglial cell population and that of the differentiated oligodendrocytes and

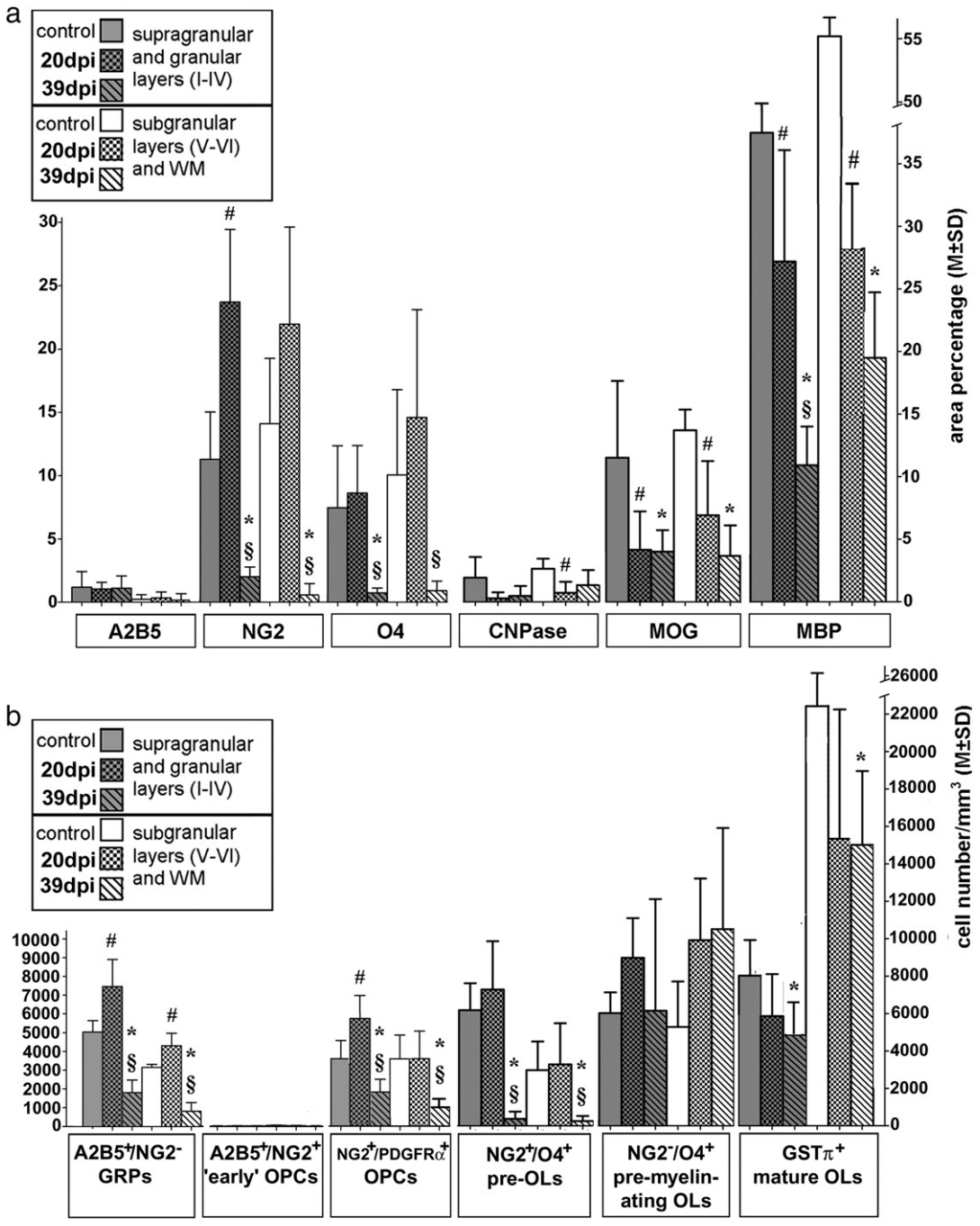

Fig. 2. Quantitative analysis in cerebral cortex supragranular/granular layers and subgranular layers/WM in healthy and EAE-affected mice at 20 and 39 dpi. (a) Tissue immunoreactivity for markers A2B5, NG2, O4, CNPase, MOG, and MBP expressed as mean percentage area ± SD. (b) Number of cells of the oligodendrocyte lineage (mean/mm^3 ± SD) identified by specific markers: A2B5$^+$/NG2$^-$ GRPs, A2B5$^+$/NG2$^+$ "transitional" OPCs, NG2$^+$/PDGFR-α$^+$ OPCs, NG2$^+$/O4$^+$ pre-oligodendrocytes, NG2$^-$/O4$^+$ pre-myelinating oligodendrocytes, GST-π$^+$ mature oligodendrocytes. One way Anova and Bonferroni post-test analyses: $p<0.05$, (#) control *vs* 20 dpi, (*) control *vs* 39 dpi, and (§) 20 dpi *vs* 39 dpi.

astrocytes, NG2/CNPase and NG2/GFAP double immunolabelings were also carried out (Supplementary Figs. 6a–f). The outcome of these stainings demonstrated that each of these three markers was restricted to a morphologically distinct cell type exhibiting a specific distribution in the cerebral cortex. In particular, the spidery, richly ramified NG2$^+$ oligodendroglial cells were clearly distinguishable from the poorly ramified and rounded CNPase$^+$ oligodendrocytes (Supplementary Figs. 6a–c), and both these oligodendrocyte types were in turn distinguishable from the typical star-like, GFAP$^+$ cortical astrocytes (Supplementary Figs. 6d–f).

Immunohistochemical analysis of myelinated fibers in cerebral cortex of EAE mice

Brain sections from EAE-affected mice sacrificed at 20 and 39 dpi, defined as "early" and "late" disease, respectively, were analyzed for the distribution of both MBP and MOG reactivity. In both stages of the disease, MBP and MOG immunoreactivity appeared significantly reduced in cerebral cortex and subcortical WM (Figs. 1a, b; 2a). In the cerebral cortex of EAE-affected mice, together with the diffuse reduction of MBP, localized areas characterized by a reduced or absent MBP reactivity were also frequently seen in the form of band-like subpial demyelination (Figs. 1a–d) and rarely as bounded lesions either extending up to layer IV (Fig. 1e), or to the subcortical WM (Fig. 1f). MBP reactivity also appeared significantly reduced in the supragranular and granular layers of mice in the "late" stage of the disease (39 dpi) as compared with the "early" stage (20 dpi) (Fig. 2a). Double stainings with anti-MBP and anti-NF antibodies were also carried out to ascertain whether the observed areas of myelin loss corresponded to primary demyelination, which is characterized by a relative sparing of axons. In EAE-affected cortex, at both 20 and 39 dpi the depletion of MBP was confirmed and NF$^+$ "naked" axons were still recognizable (Figs. 1g, h). According to the results described above, serial sections close to the detected demyelinated cortical areas were stained with the microglia/leukocyte marker CD45. In the cortex, a large population of activated microglia cells, identifiable by a low CD45 expression, was revealed together with spread macrophage-like cells, identified on the basis of a high CD45 expression (Almolda et al., 2009) (Figs. 3a, b). These CD45^{high}-reactive cells were frequently associated with demyelinating fibers (Figs. 3c, d; Supplementary Video 1) and increased during the disease course, while typical inflammatory infiltrates were never seen around cerebral cortex microvessels either at 20 dpi or at 39 dpi (Fig. 3a). These observations demonstrated that a demyelination process occurs in the cerebral cortex and subcortical WM of the analyzed EAE mice and prompted us to further investigate the distribution of oligodendrocyte lineage cells during the disease course.

Immunolocalization of cells of the oligodendrocyte lineage in EAE cerebral cortex at 20 dpi

Quantitative analysis of double immunolabeled A2B5/NG2 sections from EAE-affected mice demonstrated that the number of A2B5$^+$/NG2$^-$ GRPs was significantly increased in supragranular and granular layers, deeper subgranular layers and WM (Figs. 2b, 4a, b), the highest number of GRPs being observed in subpial cortex areas. Although the number of A2B5$^+$ GRPs was increased in EAE-affected mice, the total A2B5 staining of the cortex was not significantly different from the staining obtained in control cortex (Fig. 2a). This discrepancy could be explained by the observed reduction of the A2B5 reactivity in the EAE neuropil and

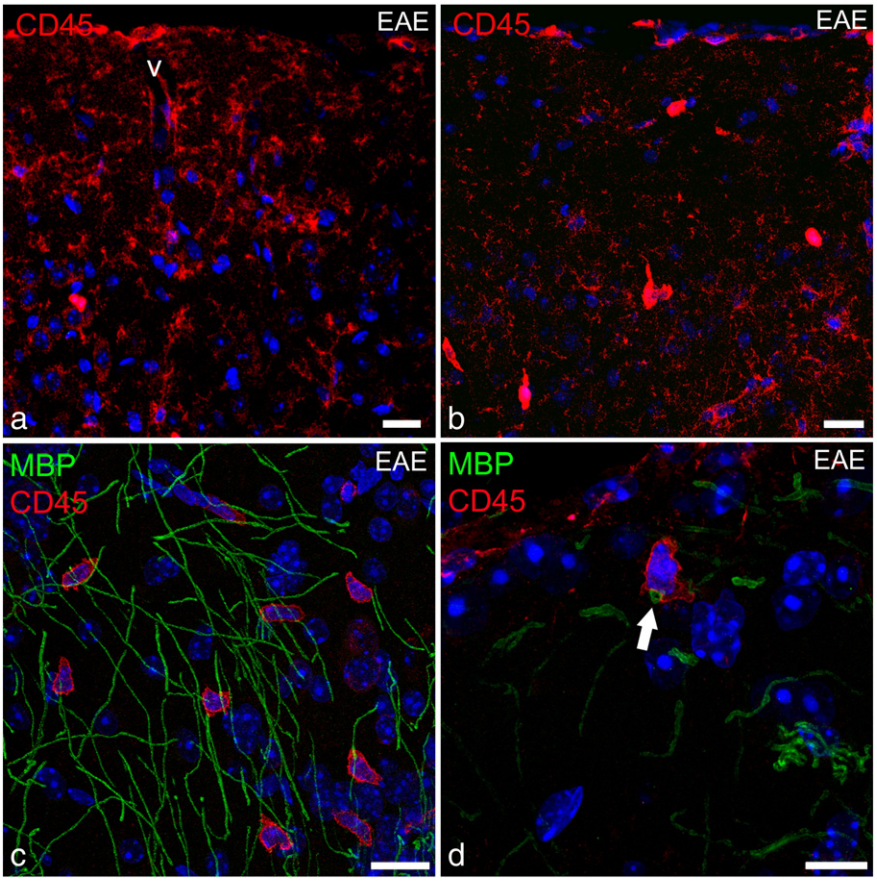

Fig. 3. Representative confocal microscopy images of EAE cerebral cortex immunolabeled for CD45 and MBP/CD45. (a, b) CD45^{low}-reactive microglia and CD45^{high}-reactive macrophage-like cells in cortex layers I and II at 20 dpi (a) and 39 dpi (b); note in a, a cortex microvessel (*v*) without signs of perivascular infiltrates. (c, d) High magnification of CD45^{high}-reactive macrophage-like cells associated with MBP-reactive fibers at 39 dpi; in d a macrophage tightly adheres to a nerve fiber (*arrow*). Scale bars: (a–c) 20 μm; (d) 10 μm.

neuron nuclei (Figs. 4a, b). As already observed in control brains, a small number of 'transitional' OPCs was also identifiable by reactivity for both A2B5 and NG2 (Fig. 2b). Double immunolabeling for the markers NG2 and O4 revealed an increase of the $NG2^+/O4^-$ OPCs in the supragranular and granular layers, whereas their number did not change in subgranular layers and WM. In EAE supragranular layers, these cells showed an immature morphology, characterized by small, rounded cell bodies, a few unbranched processes and a high level of NG2 expression (Figs. 4c–f). The observation of an OPC increase in subpial demyelinated layers was confirmed by the evaluation of their number by PDGFR-α staining (5944.68 ± 1075.04 *vs* 3705.07 ± 1113.44 cells/mm^3; $p = 0.012$; $n = 5$) (Fig. 2b; Supplementary Fig. 7), that also confirmed a steady state in deep cortex layers and WM (3750.87 ± 1261.84 *vs* 3886.52 ± 1157.92 cells/mm^3; $p = 0.86$; $n = 5$). Unlike GRPs and OPCs, the $NG2^+/O4^+$ pre-oligodendrocytes did not increase in number (Fig. 2b) but they expressed high levels of NG2 and, especially in supragranular layers, showed a deeply modified morphology characterized by an enlarged, polymorphic cell body bearing numerous dendritic-like processes (Fig. 4d). In accordance with the previous NG2 labeling results, the area of immunoreactivity for NG2 was also significantly increased in supragranular and granular layers (Fig. 2a). A slight increase of $NG2^-/O4^+$ pre-myelinating oligodendrocytes was observed in all cortical layers and WM (Figs. 2b, 4c–f) and was paralleled by the value of O4 immunoreactive cortex areas (Fig. 2a).

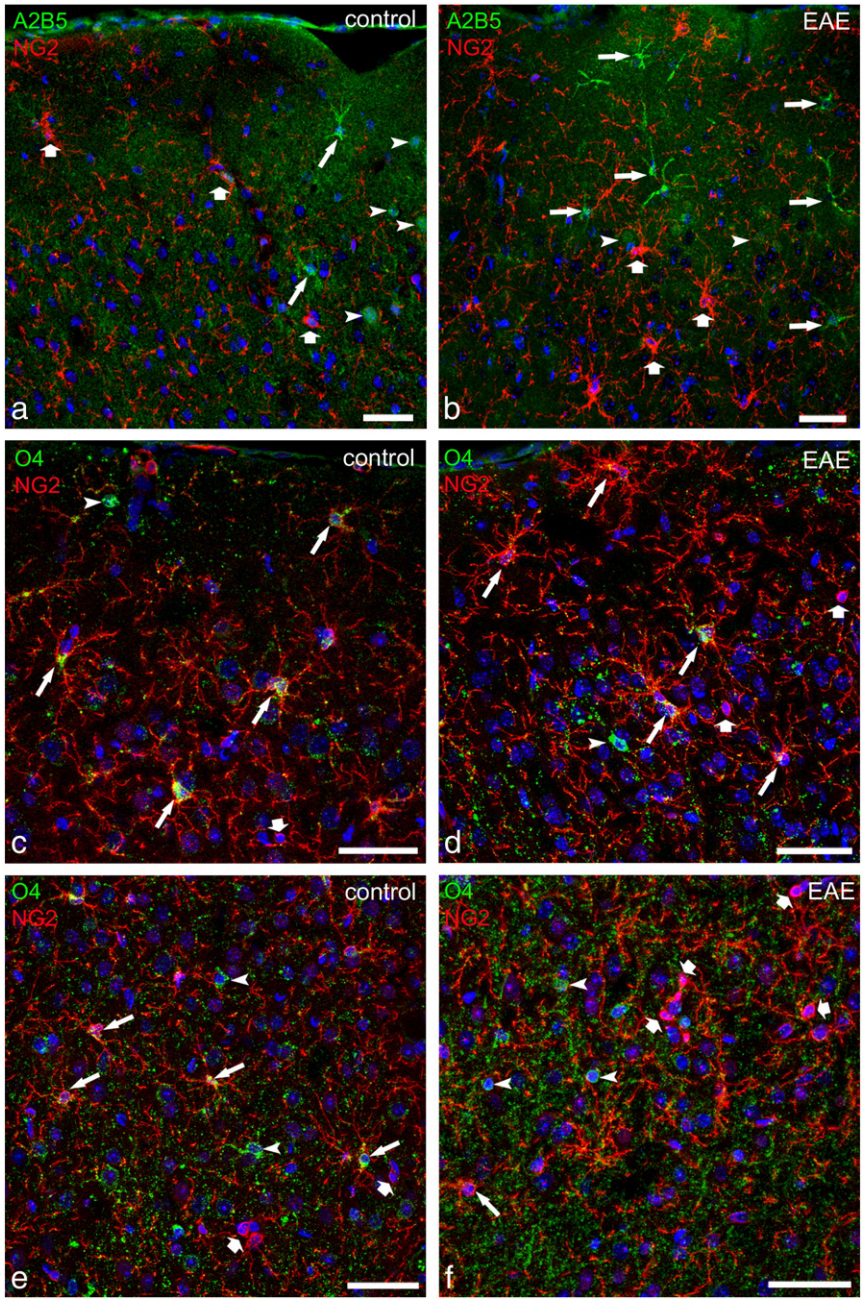

Fig. 4. Representative confocal microscopy images of control and 20 dpi EAE-affected brains immunolabeled for A2B5/NG2 and NG2/O4. (a, b) Small, scarcely ramified $A2B5^+$ GRPs (*arrows*) are significantly increased in EAE cerebral cortex supragranular and granular layers (*control* 4988.32 ± 607.4 *vs EAE* 7396.56 ± 1428.76 cell/mm^3) together with large, ramified $NG2^+$ oligodendroglial precursors (*large arrows*); *arrowheads* point to A2B5 stained neuronal nuclei. In supragranular (c, d) and granular (e, f) cortical layers, $NG2^+/O4^-$ OPCs (*large arrows*) increase significantly during EAE (*control* 3966.82 ± 957.84 *vs EAE* 6590.93 ± 1246.88 cell/mm^3), whereas $NG2^+/O4^+$ pre-oligodendrocytes (*arrows*) are numerically stable (*control* 6178.5 ± 1441.49 *vs EAE* 7284.72 ± 2579.51); $NG2^-/O4^+$ pre-myelinating oligodendrocytes (c-f, *arrowheads*), unbranched $NG2^+/O4^-$ OPCs (d, f; *large arrows*), and bushy-like $NG2^+/O4^+$ pre-oligodendrocytes (d, f; *arrows*) are also recognizable. Scale bars: 50 μm.

To ascertain a possible relation between the increase of NG2$^+$ oligodendroglial precursors and the reduced level of myelination observed in supragranular and granular cortex layers in "early EAE", we morphometrically analyzed NG2, CNPase, MOG, and MBP reactivity. As compared to the peak observed in NG2 immunoreactivity, myelin markers showed a significant reduction (Figs. 2a; 5a-f), paralleled by a non-significant decrease in the number of mature oligodendrocytes identified by GST-π (Figs. 2b; 5g, h). An additional feature of the EAE cerebral cortex was the presence of transitional NG2$^+$/CNPase$^+$ pre-myelinating oligodendrocytes (Figs. 6a–c), which were never seen in control cortex, as well as of polymorphic NG2$^+$ and O4$^+$ doublet cells (Figs. 6d–f) that are considered aspects of cell proliferation. To better evaluate the presence of an increased proliferative capacity of the oligodendrocyte precursors during "early EAE", double immunolabelings were carried out with NG2 and the proliferative marker PCNA. The analysis, performed by counting the percentage of NG2$^+$ cells marked by PCNA, revealed an increase of proliferation that, in EAE cerebral cortex, accounted for $6.02 \pm 0.91\%$ of the whole NG2$^+$ population *vs* $3.50 \pm 1.27\%$ in control brains ($p = 0.0069$; $n = 5$) (Figs. 6g, h).

Immunolocalization of cells of the oligodendrocyte lineage in EAE cerebral cortex at 39 dpi

Comparison between the observed changes in 20 dpi, "early EAE", and 39 dpi, "late EAE", demonstrated that a severe decrease in the number of precursors of the oligodendrocyte lineage took place in the "late" stage of the disease. The reduction involved A2B5$^+$/NG2$^-$ GRPs, NG2$^+$/PDGFR-α$^+$ OPCs, and NG2$^+$/O4$^+$ pre-oligodendrocytes, that showed a statistically significant decreased number as compared with those in controls and in "early" disease (Fig. 2b). In particular, the number of OPCs, that had been demonstrated to increase at 20 dpi, showed a significant reduction in 39 dpi mice, in both supragranular and granular cerebral cortex layers (1884.03 ± 804.96 *vs* 5944.68 ± 1075.04; $p = 0.0001$; $n = 5$) and subgranular layers and WM (1118.48 ± 397.95 *vs* 3750.87 ± 1261.84; $p = 0.0021$; $n = 5$) (Fig. 2b). A significant reduction of mature GST-π$^+$ oligodendrocytes was also observed as compared to controls, and was paralleled by a further decrease of MOG and MBP immunoreactivity (Figs. 2a, b). Among the different types of immature and mature oligodendrocytes, only the differentiated NG2$^-$/O4$^+$ pre-myelinating oligodendrocytes did not appear quantitatively reduced (Fig. 2b). Overall, these data indicated that in "late EAE" the main observed changes consisted of a progressive process of demyelination together with an arrest of oligodendrocyte precursors proliferation.

Discussion

Neocortical lesions have long been recognized to be present in MS (Brownell and Hughes, 1962; Greenfield and King, 1936) and to be prominent in patients with progressive MS (Bø et al., 2003; Geurts et al., 2009; Kidd et al., 1999). In the past decade, only few, specifically modeled EAE experiments have demonstrated a cortical involvement similar to that seen in MS in humans (Merkler et al., 2006; Pomeroy et al., 2005; Storch et al., 2006), while conventional MOG-induced EAE in C57BL/6 mice has been extensively studied and has not previously been documented to display grey matter lesions (Kim et al., 2010; Zamvil and Steinman, 1990), even if in this model indirect evidence of cerebral cortex disease has been suggested (Tu et al., 2009; Zeis et al., 2008). Recently, the histopathological bases of inflammation and demyelination in the cerebral cortex and corpus callosum have been described in chronic EAE induced by MOG peptide 35–55 in C57BL/6 mice (Mangiardi et al., 2011). Interestingly, in this study demyelinating lesions located in different areas of the cerebral cortex, as well as structural and functional alterations, have been demonstrated to mimic cortical and callosal pathologic abnormalities of progressive MS. Our study confirms the presence of cerebral cortex demyelinating lesions in the standard MOG-induced EAE mouse model and extends the analysis to the changes that involve the oligodendrocyte cell lineage. Areas of subpial demyelination were disclosed in the form of band-like diffuse myelin reduction and as bounded areas resembling the general subpial demyelination, type III and type IV lesions described in the cerebral cortex of progressive MS patients (Bø et al., 2003; Geurts et al., 2005; Peterson et al., 2001). In cortical lesions of progressive MS, signs of remyelination have also been shown (Albert et al., 2007; Patani et al., 2007), however, the immunomorphological criteria adopted in this study do not allow us to distinguish between partially demyelinated and remyelinating fibers, making it impossible to establish whether new wrapping of demyelinated axons occurs during the phases of the disease under study. As recently demonstrated, new molecular markers of demyelination/remyelination are needed to specifically identify the ongoing processes (Ma et al., 2011).

Thereafter, we identified and quantitatively evaluated, on the basis of the study carried out on control brains with a broad panel of oligodendrocyte markers, the morphological and quantitative changes that occur in the cells of the oligodendrocyte lineage in EAE-affected brains. In the control cerebral cortex and subcortical WM, virtually all the cells of the oligodendrocyte lineage are identified by their morphology and antigenic phenotype (Supplementary Fig. 8), the prevalent population being OPCs/polydendrocytes. Other numerically considerable precursors were GRPs and pre-oligodendrocytes; the former have previously been revealed in the developing brain and are considered as early progenitors of the oligo-astroglia cell lineage (Liu et al., 2002; Strathmann et al., 2007). As demonstrated in the developing murine cerebral cortex, the subpial area is an additional niche for oligodendrogenesis (Costa et al., 2007). At this site, the oligodendrogenesis that takes place in adulthood may be reactivated in EAE conditions and evidence for this reactivation may be afforded by the increment of GRPs.

Based upon the outcome of our phenotypical study, the large population of NG2$^+$ cells includes the classically described OPCs/polydendrocytes, which also show specific reactivity for PDGFR-α, and encompasses a subset of pre-oligodendrocytes identified by their coincident O4 expression. In "early EAE", NG2$^+$ oligodendroglial cells seem to react to demyelination by pronounced proliferation. The proliferative response of NG2$^+$ cells has been reported in previous studies (Di Bello et al., 1999; Keirstead et al., 1998; Polito and Reynolds, 2005; Reynolds et al., 2002) and has been suggested to be promoted by interactions of NG2 with non-myelinated axons (Kucharova and Stallcup, 2010). In our model, the proliferative attitude of NG2$^+$ cells is suggested by the presence of NG2$^+$ doublet cells, deemed to be dividing cells that maintain a differentiated morphology (Ge et al., 2009; Kukley et al., 2008), and is confirmed by morphometric analysis of proliferating precursors identified by NG2/PCNA markers. In "early EAE", proliferation of NG2$^+$ cells in cerebral cortex increases two-fold in the subpial cortex layers, where a more evident and extended demyelination has also been demonstrated. The emerging data on proliferation and differentiation capacities of OPCs endorse the concept of a fundamental contribution of these cells to CNS plasticity under physiological conditions and during remyelination (Staugaitis and Trapp, 2009; Tripathi et al., 2010; Zawadzka et al., 2010; Zhu et al., 2011). As compared with other precursors of the glial lineage, OPCs, which are present both during brain development and in adulthood, are extremely plastic and may respond to the neural microenviroment by exerting multiple functions, as well as resuming their proliferative capability (Mangin and Gallo, 2011; Simon et al., 2011; Wigley et al., 2007). In this view, it is conceivable that during the early phase of MS, proliferation of OPCs may occur as a response to short-lasting demyelination, initiating, together with other mechanisms such as the release of anti-inflammatory cytokines and redistribution of axon channels, a repair process (Chang et al., 2000; Hollifield et al., 2003; Moll et al., 1991). Unlike OPCs, NG2$^+$/O4$^+$ pre-oligodendrocytes

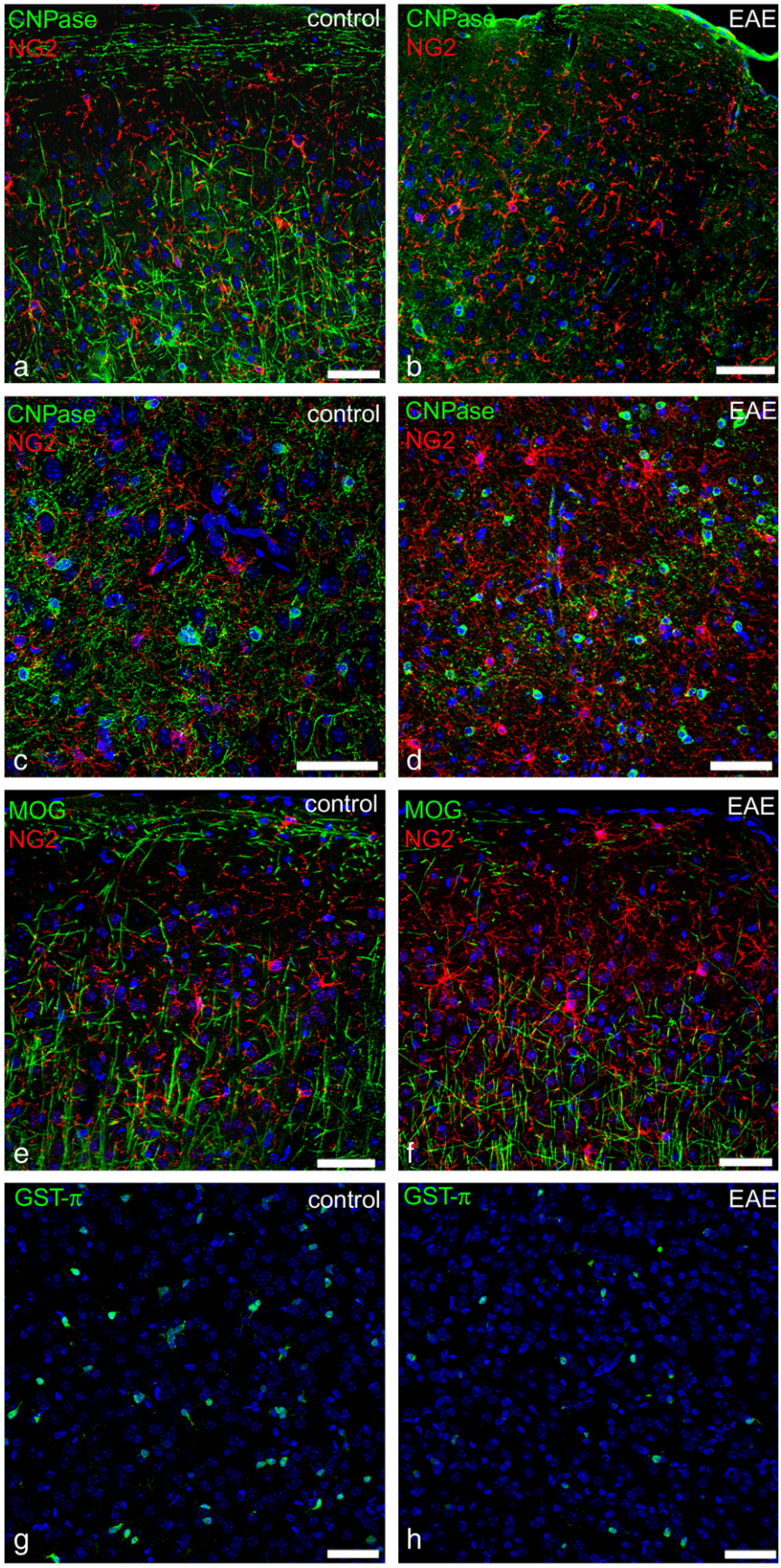
CNPase
NG2
control
a
CNPase
NG2
EAE
b
CNPase
NG2
control
c
CNPase
NG2
EAE
d
MOG
NG2
control
e
MOG
NG2
EAE
f
GST-π
control
g
GST-π
EAE
h

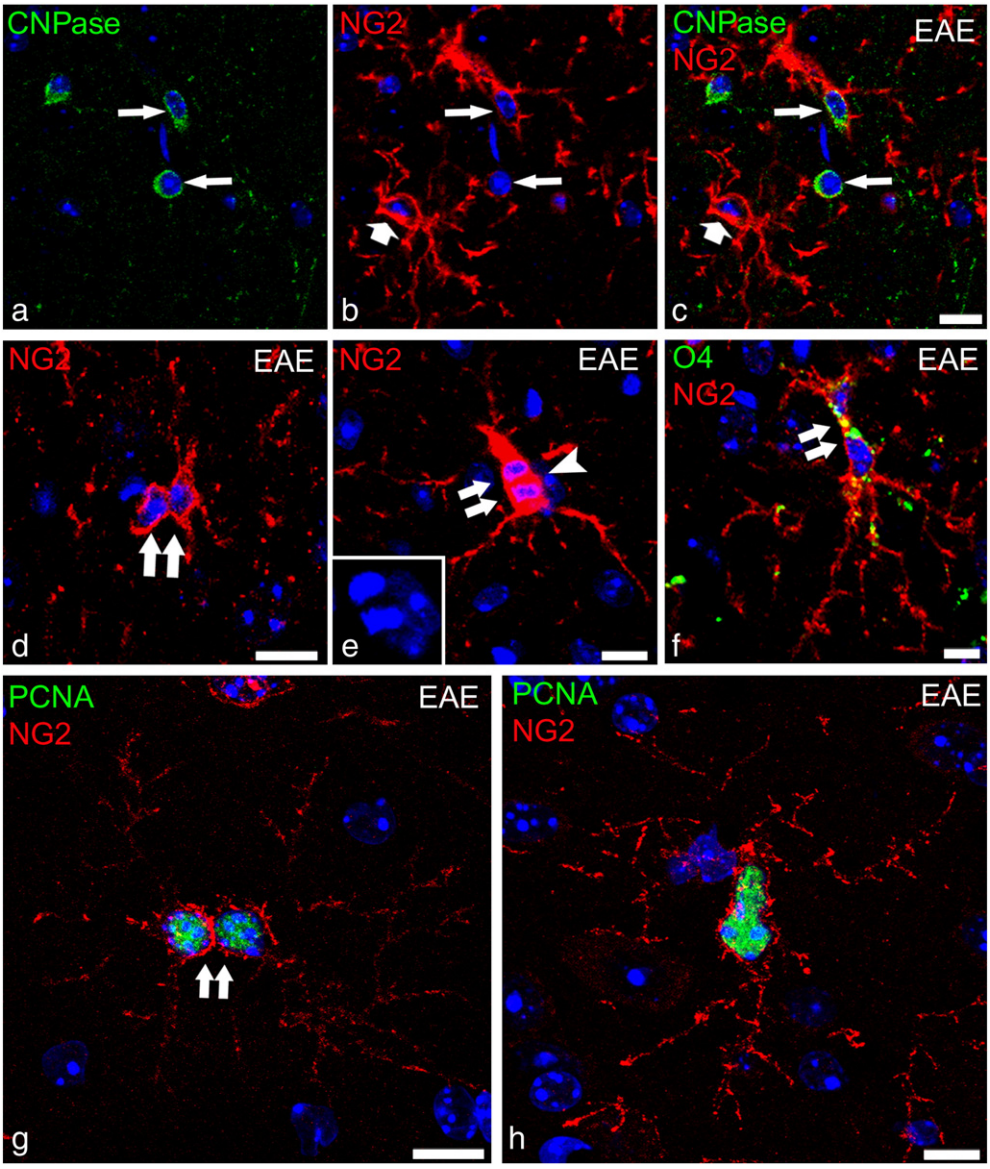

Fig. 6. Representative confocal microscopy images of EAE cerebral cortex at 20 dpi immunolabeled for NG2 also combined with CNPase, O4, and PCNA. Single channels (a, b) and merged image (c) of NG2$^+$/CNPase$^+$ transitional pre-myelinating oligodendrocytes (*arrows*) together with an NG2$^+$ oligodendroglial precursor (*large arrow* in b and c). (d, e) NG2$^+$ doublet cells (*double arrow*), note in e the dividing nucleus (*arrowhead*, better shown in the *inset*). (f) A doublet cell showing an NG2$^+$/O4$^+$ pre-oligodendrocyte phenotype (*double arrow*). (g, h) NG2$^+$ oligodendrocyte precursors labeled by PCNA (note in g a doublet cell, *double arrow*) as examples of this proliferating population (*control* 3.50 ± 1.27% *vs EAE* 6.02 ± 0.91%). Scale bars: 15 μm.

remain numerically stable and seem to respond to the cortex damage by acquiring a hypertrophic, reactive morphology; traces of their differentiation are revealed by the appearance of an NG2$^+$/CNPase$^+$ transitional phenotype. In "early EAE", despite the proliferative response of OPCs to the demyelinating damage, the mature GST-π$^+$ oligodendrocytes show a tendency to reduce and have been suggested to be unable to resume the myelination program (Keirstead and Blakemore, 1997).

It is known that cultured OPCs undergo a finite number of cell divisions, after which they differentiate into more mature oligodendrocytes, even when proliferative stimuli are provided in excess (Noble et al., 1988; Raff et al., 1988). In fact, in the "late" disease, when the process of demyelination becomes more evident, the proliferation potential of precursors seems to become exhausted and an overwhelming loss of the entire oligodendrocyte lineage takes place. The number of oligodendrocyte precursors significantly declines along with that of mature myelinating oligodendrocytes, while pre-myelinating oligodendrocytes seem to be the only cell type that remains numerically stable. This can be explained by considering that at least a subset of the OPCs present at the "early" stage of the disease may embark upon a differentiation program to generate, in "late EAE", the population of pre-myelinating oligodendrocytes that, however,

Fig. 5. Representative confocal microscopy images of control and 20 dpi EAE-affected brains immunolabeled for NG2/CNPase, NG2/MOG, and GST-π. In supragranular (a, b) and granular (c, d) cortex layers, CNPase$^+$ myelinated fibers diminish in EAE, whereas CNPase$^+$ oligodendrocyte bodies are still in place; (e, f) a similar degree of demyelination is also shown with MOG, together with a prominent network of NG2$^+$ oligodendroglial precursors. (g, h) When compared with controls, the number of GST-π$^+$ oligodendrocyte bodies is decreased in both EAE cortex and subcortical WM (supragranular and granular layers: *control* 8252.26 ± 1582.27 *vs EAE* 6067.12 ± 1976.91 cell/mm^3; subgranular layers and WM: *control* 24992.85 ± 874.86 *vs EAE* 15276.27 ± 8293.68 cell/mm^3). Scale bars: 50 μm.

appears to be unable to sustain the decreasing population of mature oligodendrocytes.

Different mechanisms have been suggested to sustain the MS/EAE pathogenesis and outcome, including a reduction of differentiation-inducing signals, the presence of local inhibitors of oligodendrocyte differentiation and/or axon-wrapping capacities (Butovsky et al., 2006; Chen et al., 2009; Höftberger et al., 2010; Huang et al., 2011; Jurynczyk et al., 2008; Kremer et al., 2011; Mi et al., 2005), modified interactions with the dystrophic axons (Chang et al., 2002; John et al., 2002). In this context, our results confirm that a defect in the differentiation program may specifically intervene in critical steps of oligodendrocyte maturative progression (Kuhlmann et al., 2008), and pinpoint the maturational block in a late differentiation stage, possibly coinciding with pre-myelinating oligodendrocytes.

Overall, the observations carried out in this chronic EAE model identify a two-phase response of oligodendrocyte precursors, provide an additional phenomenological basis for a better understanding of the pathogenesis of progressive MS, and suggest the proliferative response of OPCs during "early EAE" as a potential for remyelination, as well as offering indications underlining the importance of implementing early therapeutic strategies aimed at impeding the progression to extensive demyelination.

Supplementary materials related to this article can be found online at doi:10.1016/j.nbd.2011.05.021.

Acknowledgments

Prof. H.E. de Vries (Dept. of Molecular and Cell Biology and Immunology, VU University Medical Center, Amsterdam, The Netherlands) is greatly acknowledged for her critical review of the manuscript. We would like to thank M.V.C. Pragnell, BA, for linguistic help. This work was supported by a grant from Regione Puglia (Italy) Neurobiotech (Progetto Strategico PS124, 2006) to L.R., Fondazione Cassa di Risparmio di Puglia, (FCRP 2010) to D.V.; in part by intramural fund from the University of Bari (2009) to D.V. and from the Italian Ministry of the University and Scientific Research (MIUR), PRIN 2008 to R.P. and L.R.

References

Albert, M., Antel, J., Brück, W., Stadelmann, C., 2007. Extensive cortical remyelination in patients with chronic multiple sclerosis. Brain Pathol 17, 129–138.
Almolda, B., Costa, M., Montoya, M., González, B., Castellano, B., 2009. CD4 microglial expression correlates with spontaneous clinical improvement in the acute Lewis rat EAE model. J. Neuroimmunol. 209, 65–80.
Bansal, R., Warrington, A.E., Gard, A., Ranscht, B., Pfeiffer, S.E., 1989. Multiple and novel specificities of monoclonal antibodies O1, O4 and R-Mab used in the analysis of oligodendrocyte development. J. Neurosci. Res. 24, 548–557.
Baumann, N., Pham-Dihn, D., 2001. Biology of oligodendrocyte and myelin in the mammalian Central Nervous System. Physiol. Rev. 81, 871–927.
Berard, J.L., Wolak, K., Fournier, S., David, S., 2010. Characterization of relapsing–remitting and chronic forms of experimental autoimmune encephalomyelitis in C57BL/6 mice. Glia 58, 434–445.
Blakemore, W.F., 1974. Pattern of remyelination in the CNS. Nature 249, 577–578.
Bø, L., 2009. The histopathology of grey matter demyelination in multiple sclerosis. Acta Neurol Scand Suppl 189, 51–57.
Bø, L., Vedeler, C.A., Nyland, H.I., Trapp, B.D., Mørk, S.J., 2003. Subpial demyelination in the cerebral cortex of multiple sclerosis patients. J. Neuropathol. Exp. Neurol. 62, 723–732.
Brownell, B., Hughes, J.T., 1962. The distribution of plaques in the cerebrum in multiple sclerosis. J Neurol Neurosurg Psychiatry 25, 315–320.
Bunge, M.B., Bunge, R.P., Ris, H., 1961. Ultrastructural study of remyelination in an experimental lesion in adult cat spinal cord. J Biophys Biochem Cyto 10, 67–94.
Butovsky, O., Landa, G., Kunis, G., Ziv, Y., Avidan, H., Greenberg, N., et al., 2006. Induction and blockage ofoligodendrogenesis by differently activated microglia in an animal model of multiple sclerosis. J Clin Invest 116, 905–915.
Butt, A.M., Hamilton, N., Hubbard, P., Pugh, M., Ibrahim, M., 2005. Synantocytes: the fifth element. J. Anat. 207, 695–706.
Cai, Z., Lin, S., Fan, L.W., Pang, Y., Rhodes, P.G., 2006. Minocycline alleviates hypoxic-ischemic injury to developing oligodendrocytes in the neonatal rat brain. Neuroscience 137, 425–435.
Cameron, R.S., Rakic, P., 1991. Glial cell lineage in the cerebral cortex: a review and synthesis. Glia 4, 124–137.
Chang, A., Nishiyama, A., Peterson, J., Prineas, J., Trapp, B.D., 2000. NG2-positive oligodendrocyte progenitor cells in adult human brain and multiple sclerosis lesions. J. Neurosci. 20, 6404–6412.
Chang, A., Tourtellotte, W.W., Rudick, R., Trapp, B.D., 2002. Premyelinating oligodendrocytes in chronic lesions of multiple sclerosis. New Engl J Med 346, 165–173.
Chekenya, M., Krakstad, C., Svendsen, A., Netland, I.A., Staalesen, V., Tysnes, B.B., et al., 2008. The progenitor cell marker NG2/MPG promotes chemoresistance by activation of integrin-dependent PI3K/Akt signaling. Oncogene 27, 5182–5194.
Chen, J.T., Narayanan, S., Collins, D.L., Smith, S.M., Matthews, P.M., Arnold, D.L., 2004. Relating neocortical pathology to disability progression in multiple sclerosis using MRI. NeuroImage 23, 1168–1175.
Chen, Y., Wu, H., Wang, S., Koito, H., Li, J., Ye, F., et al., 2009. The oligodendrocyte-specific G protein-coupled receptor GPR17 is a cell-intrinsic timer of myelination. Nat. Neurosci. 12, 1398–1406.
Costa, M.R., Kessaris, N., Richardson, W.D., Götz, M., Hedin-Pereira, C., 2007. The marginal zone/layer I as a novel niche for neurogenesis and gliogenesis in developing cerebral cortex. J. Neurosci. 27, 11376–11388.
De Stefano, N., Matthews, P.M., Filippi, M., Agosta, F., De Luca, M., Bartolozzi, M.L., et al., 2003. Evidence of early cortical atrophy in MS: relevance to white matter changes and disability. Neurology 60, 1157–1162.
Di Bello, I.C., Dawson, M.R.L., Levine, J.M., Reynolds, R., 1999. Generation of oligodendroglial progenitors in acute inflammatory demyelinating lesions of the rat brain stem is stimulated by demyelination rather than inflammation. J. Neurocytol. 28, 365–381.
Franklin, R.J., ffrench-Constant, C., 2008. Remyelination in the CNS: from biology to therapy. Nat. Rev. Neurosci. 9, 839–855.
Frohman, E.M., Racke, M.K., Raine, C.S., 2006. Multiple sclerosis—the plaque and its pathogenesis. N Engl J Med 354, 942–955.
Fruttiger, M., Karlsson, L., Hall, A.C., Abramsson, A., Calver, A.R., Boström, H., et al., 1999. Defective oligodendrocyte development and severe hypomyelination in PDGF-A knockout mice. Development 126, 457–467.
Ge, W.P., Zhou, W., Luo, Q., Jan, L.Y., Jan, Y.N., 2009. Dividing glial cells maintain differentiated properties including complex morphology and functional synapses. Proc Natl Acad Sci U S A 106, 328–333.
Gensert, J.M., Goldman, J.E., 1997. Endogenous progenitors remyelinate demyelinated axons in the adult CNS. Neuron 19, 197–203.
Geurts, J.J., Bö, L., Pouwels, P.J., Castelijns, J.A., Polman, C.H., Barkhof, F., 2005. Cortical lesions in multiple sclerosis: combined postmortem MR imaging and histopathology. AJNR Am J Neuroradiol 26, 572–577.
Geurts, J.J., Stys, P.K., Minagar, A., Amor, S., Zivadinov, R., 2009. Gray matter pathology in (chronic) MS: modern views on an early observation. J. Neurol. Sci. 282, 12–20.
Gold, R., Linington, C., Lassmann, H., 2006. Understanding pathogenesis and therapy of multiple sclerosis via animal models: 70 years of merits and culprits in experimental autoimmune encephalomyelitis research. Brain 129, 1953–1971.
Goldman, J.E., 2005. Lineages of astrocytes and oligodendrocytes, In: Kettenmann, H., Ransom, B.R. (Eds.), Neuroglia, 2nd edn. Oxford University Press, New York, pp. 72–84.
Goldschmidt, T., Antel, J., König, F.B., Brück, W., Kuhlmann, T., 2009. Remyelination capacity of the MS brain decreases with disease chronicity. Neurology 72, 1914–1921.
Greenfield, J.G., King, L.S., 1936. Observations on the histopathology of the cerebral lesions in disseminated sclerosis. Brain 59, 445–458.
Guardia Clausi, M., Pasquini, L.A., Soto, E.F., Pasquini, J.M., 2010. Apotransferrin-induced recovery after hypoxic/ischaemic injury on myelination. ASN Neuro 2, e00048.
He, Y., Cai, W., Wang, L., Chen, P., 2009. A developmental study on the expression of PDGFalphaR immunoreactive cells in the brain of postnatal rats. Neurosci. Res. 65, 272–279.
Heldin, C.H., Westermark, B., 1999. Mechanism of action and in vivo role of platelet-derived growth factor. Physiol. Rev. 79, 1283–1316.
Höftberger, R., Fink, S., Aboul-Enein, F., Botond, G., Olah, J., Berki, T., et al., 2010. Tubulin polymerization promoting protein (TPPP/p25) as a marker for oligodendroglial changes in multiple sclerosis. Glia 58, 1847–1857.
Hollifield, R.D., Harbige, L.S., Pham-Dinh, D., Sharief, M.K., 2003. Evidence for cytokine dysregulation in multiple sclerosis: peripheral blood mononuclear cell production of pro-inflammatory and anti-inflammatory cytokines during relapse and remission. Autoimmunity 36, 133–141.
Huang, J.K., Jarjour, A.A., Nait Oumesmar, B., Kerninon, C., Williams, A., Krezel, W., et al., 2011. Retinoid X receptor gamma signaling accelerates CNS remyelination. Nat. Neurosci. 14, 45–53.
John, G.R., Shankar, S.L., Shafit-Zagardo, B., Massimi, A., Lee, S.C., Raine, C.S., et al., 2002. Multiple sclerosis: re-expression of a developmental pathway that restricts oligodendrocyte maturation. Nat Med 8, 1115–1121.
Jurynczyk, M., Jurewicz, A., Bielecki, B., Raine, C.S., Selmaj, K., 2008. Overcoming failure to repair demyelination in EAE: gamma-secretase inhibition of Notch signaling. J. Neurol. Sci. 265, 5–11.
Keirstead, H.S., Blakemore, W.F., 1997. Identification of post-mitotic oligodendrocytes incapable of remyelination within the demyelinated adult spinal cord. J. Neuropathol. Exp. Neurol. 56, 1191–1201.
Keirstead, H.S., Levine, J.M., Blakemore, W.F., 1998. Response of the oligodendrocyte progenitor cell population (defined by NG2 labelling) to demyelination of the adult spinal cord. Glia 22, 161–170.
Kidd, D., Barkhof, F., McConnell, R., Algra, P.R., Allen, I.V., Revesz, T., 1999. Cortical lesions in multiple sclerosis. Brain 122, 17–26.
Kim, J.V., Jiang, N., Tadokoro, C.E., Liu, L., Ransohoff, R.M., Lafaille, J.J., et al., 2010. Two-photon laser scanning microscopy imaging of intact spinal cord and cerebral cortex reveals requirement for CXCR6 and neuroinflammation in immune cell infiltration of cortical injury sites. J Immunol Methods 352, 89–100.
Kremer, D., Aktas, O., Hartung, H.P., Küry, P., 2011. The complex world of oligodendroglial differentiation inhibitors. Ann. Neurol. 69, 602–618.
Kucharova, K., Stallcup, W.B., 2010. The NG2 proteoglycan promotes oligodendrocyte progenitor proliferation and developmental myelination. Neuroscience 166, 185–194.

Kuhlmann, T., Miron, V., Cui, Q., Wegner, C., Antel, J., Brück, W., 2008. Differentiation block of oligodendroglial progenitor cells as a cause for remyelination failure in chronic multiple sclerosis. Brain 131, 1749–1758.
Kukley, M., Kiladze, M., Tognatta, R., Hans, M., Swandulla, D., Schramm, J., et al., 2008. Glial cells are born with synapses. FASEB J. 22, 2957–2969.
Kundu, S.K., Pleatman, M.A., Redwine, W.A., Boyd, A.E., Marcus, D.M., 1983. Binding of monoclonal antibody A2B5 to gangliosides. Biochem. Biophys. Res. Commun. 116, 836–842.
Kutzelnigg, A., Lucchinetti, C.F., Stadelmann, C., Brück, W., Rauschka, H., Bergmann, M., et al., 2005. Cortical demyelination and diffuse white matter injury in multiple sclerosis. Brain 128, 2705–2712.
Lassmann, H., Brück, W., Lucchinetti, C., Rodriguez, M., 1997. Remyelination in multiple sclerosis. Mult. Scler. 3, 133–136.
Lazeron, R.H., Langdon, D.W., Filippi, M., van Waesberghe, J.H., Stevenson, V.L., Boringa, J.B., et al., 2000. Neuropsychological impairment in multiple sclerosis patients: the role of (juxta) cortical lesion on FLAIR. Mult. Scler. 6, 280–285.
Ledeen, R.W., Wu, G., 2008. Nuclear sphingolipids: metabolism and signaling. J Lipid Res 49, 1176–1186.
Levine, J.M., Stincone, F., Lee, Y.S., 1993. Development and differentiation of glial precursor cells in the rat cerebellum. Glia 7, 307–321.
Liu, Y., Wu, Y., Lee, J.C., Xue, H., Pevny, L.H., Kaprielian, Z., et al., 2002. Oligodendrocyte and astrocyte development in rodents: an in situ and immunohistological analysis during embryonic development. Glia 40, 25–43.
Lucchinetti, C., Bruck, W., Parisi, J., Scheithauer, B., Rodriguez, M., Lassmann, H., 2000. Heterogeneity of multiple sclerosis lesions: implications for the pathogenesis of demyelination. Ann. Neurol. 47, 707–717.
Ma, J., Tanaka, K.F., Shimizu, T., Bernard, C.C., Kakita, A., Takahashi, H., et al., 2011. Microglial cystatin F expression is a sensitive indicator for ongoing demyelination with concurrent remyelination. J. Neurosci. Res. 89, 639–649.
Makagiansar, I.T., Williams, S., Mustelin, T., Stallcup, W.B., 2007. Differential phosphorylation of NG2 proteoglycan by ERK and PKCalpha helps balance cell proliferation and migration. J Cell Biol 178, 155–165.
Mangiardi, M., Crawford, D.K., Xia, X., Du, S., Simon-Freeman, R., Voskuhl, R.R., et al., 2011. An animal model of cortical and callosal pathology in multiple sclerosis. Brain Pathol 21, 263–278.
Mangin, J.M., Gallo, V., 2011. The curious case of NG2 cells: transient trend or game changer? ASN Neuro 3 pii:e00052.
Merkler, D., Ernsting, T., Kerschensteiner, M., Brück, W., Stadelmann, C., 2006. A new focal EAE model of cortical demyelination: multiple sclerosis-like lesions with rapid resolution of inflammation and extensive remyelination. Brain 129, 1972–1983.
Mi, S., Miller, R.H., Lee, X., Scott, M.L., Shulag-Morskaya, S., Shao, Z., et al., 2005. LINGO-1 negatively regulates myelination by oligodendrocytes. Nat. Neurosci. 8, 745–751.
Moll, C., Mourre, C., Lazdunski, M., Ulrich, J., 1991. Increase of sodium channels in demyelinated lesions of multiple sclerosis. Brain Res 556, 311–316.
Nishiyama, A., Lin, X.H., Giese, N., Heldin, C.H., Stallcup, W.B., 1996. Interaction between NG2 proteoglycan and PDGF alpha-receptor on O2A progenitor cells is required for optimal response to PDGF. J. Neurosci. Res. 43, 315–330.
Nishiyama, A., Komitova, M., Suzuki, R., et al., 2009. Polydendrocytes (NG2 cells): multifunctional cells with lineage plasticity. Nat. Rev. Neurosci. 10, 9–22.
Noble, M., Murray, K., Stroobant, P., Waterfield, M.D., Riddle, P., 1988. Platelet-derived growth factor promotes division and motility and inhibits premature differentiation of the oligodendrocyte/type-2 astrocyte progenitor cell. Nature 333, 560–562.
Papadopoulos, D., Rundle, J., Patel, R., Marshall, I., Stretton, J., Eaton, R., et al., 2010. FTY720 ameliorates MOG-induced experimental autoimmune encephalomyelitis by suppressing both cellular and humoral immune responses. J. Neurosci. Res. 88, 346–359.
Patani, R., Balaratnam, M., Vora, A., Reynolds, R., 2007. Remyelination can be extensive in multiple sclerosis despite a long disease course. Neuropathol. Appl. Neurobiol. 33, 277–287.
Patrikios, P., Stadelmann, C., Kutzelnigg, A., Rauschka, H., Schmidbauer, M., Laursen, H., et al., 2006. Remyelination is extensive in a subset of multiple sclerosis patients. Brain 129, 3165–3172.
Peterson, J.W., Bø, L., Mörk, S.J., Chang, A., Trapp, B.D., 2001. Transected neurites, apoptotic neurons, and reduced inflammation in cortical multiple sclerosis lesions. Ann. Neurol. 50, 389–400.
Polito, A., Reynolds, R., 2005. NG2-expressing cells as oligodendrocyte progenitors in the normal and demyelinated adult central nervous system. J. Anat. 207, 707–716.
Pomeroy, I.M., Matthews, P.M., Frank, J.A., Jordan, E.K., Esiri, M.M., 2005. Demyelinated neocortical lesions in marmoset autoimmune encephalomyelitis mimic those in multiple sclerosis. Brain 128, 2713–2721.
Prineas, J.W., Barnard, R.O., Kwon, E.E., Sharer, L.R., Cho, E.S., 1993. Multiple sclerosis: remyelination of nascent lesions. Ann. Neurol. 33, 137–151.
Probstmeier, R., Michels, M., Franz, T., Chan, B.M., Pesheva, P., 1999. Tenascin-R interferes with integrin-dependent oligodendrocyte precursor cell adhesion by a ganglioside-mediated signalling mechanism. Eur. J. Neurosci. 11, 2474–2488.
Quarles, R.H., 1997. Glycoprotein of myelin sheaths. J. Mol. Neurosci. 8, 1–12.
Raff, M.C., Lillien, L.E., Richardson, W.D., Burne, J.F., Noble, M.D., 1988. Platelet-derived growth factor from astrocytes drives the clock that times oligodendrocyte development in culture. Nature 333, 562–565.
Rasmussen, S., Wang, Y., Kivisäkk, P., Bronson, R.T., Meyer, M., Imitola, J., et al., 2007. Persistent activation of microglia is associated with neuronal dysfunction of callosal projecting pathways and multiple sclerosis-like lesions in relapsing–remitting experimental autoimmune encephalomyelitis. Brain 130, 2816–2829.
Reynolds, R., Dawson, M., Papadopoulos, D., Polito, A., Di Bello, I.C., Pham-Dinh, D., et al., 2002. The response of NG2-expressing oligodendrocyte progenitors to demyelination in MOG-EAE and MS. J. Neurocytol. 31, 523–536.
Rudick, R.A., Trapp, B.D., 2009. Gray-matter injury in multiple sclerosis. N Engl J Med 361, 1505–1506.
Simon, C., Götz, M., Dimou, L., 2011. Progenitors in the adult cerebral cortex: cell cycle properties and regulation by physiological stimuli and injury. Glia 59, 869–881.
Sommer, I., Schachner, M., 1981. Monoclonal antibodies (01 to 04) to oligodendrocyte cell surfaces: an immunocytological study in the central nervous system. Dev. Biol. 83, 311–327.
Stadelmann, C., Albert, M., Wegner, C., Brück, W., 2008. Cortical pathology in multiple sclerosis. Curr. Opin. Neurol. 21, 229–234.
Staugaitis, S.M., Trapp, B.D., 2009. NG2-positive glia in the human central nervous system. Neuron Glia Biol 5, 35–44.
Steiner, J., Bernstein, H.G., Bielau, H., Berndt, A., Brisch, R., Mawrin, C., et al., 2007. Evidence for a wide extra-astrocytic distribution of S100B in human brain. BMC Neurosci. 8, 2.
Storch, M.K., Bauer, J., Linington, C., Olsson, T., Weissert, R., Lassmann, H., 2006. Cortical demyelination can be modeled in specific rat models of autoimmune encephalomyelitis and is major histocompatability complex (MHC) haplotype-related. J. Neuropathol. Exp. Neurol. 65, 1137–1142.
Strathmann, F.G., Wang, X., Mayer-Pröschel, M., 2007. Identification of two novel glial-restricted cell populations in the embryonic telencephalon arising from unique origins. BMC Dev. Biol. 7, 33.
Tansey, F.A., Cammer, W., 1991. A pi form of glutathione-S-transferase is a myelin- and oligodendrocyte-associated enzyme in mouse brain. J. Neurochem. 57, 95–102.
Tripathi, R.B., Rivers, L.E., Young, K.M., Jamen, F., Richardson, W.D., 2010. NG2 glia generate new oligodendrocytes but few astrocytes in a murine experimental autoimmune encephalomyelitis model of demyelinating disease. J. Neurosci. 30, 16383–16390.
Tu, J.L., Zhao, C.B., Vollmer, T., Coons, S., Lin, H.J., Marsh, S., et al., 2009. APOE 4 polymorphism results in early cognitive deficits in an EAE model. Biochem. Biophys. Res. Commun. 384, 466–470.
Wigley, R., Hamilton, N., Nishiyama, A., Kirchhoff, F., Butt, A.M., 2007. Morphological and physiological interactions of NG2-glia with astrocytes and neurons. J. Anat. 210, 661–670.
Wolswijk, G., 1998. Chronic stage multiple sclerosis lesions contain a relatively quiescent population of oligodendrocyte precursor cells. J. Neurosci. 18, 601–609.
Wolswijk, G., 2002. Oligodendrocyte precursor cells in the demyelinated multiple sclerosis spinal cord. Brain 125, 338–349.
Zamvil, S.S., Steinman, L., 1990. The T lymphocyte in experimental allergic encephalomyelitis. Annu. Rev. Immunol. 8, 579–621.
Zawadzka, M., Rivers, L.E., Fancy, S.P., Zhao, C., Tripathi, R., Jamen, F., et al., 2010. CNS-resident glial progenitor/stem cells produce Schwann cells as well as oligodendrocytes during repair of CNS demyelination. Cell Stem Cell 6, 578–590.
Zeis, T., Kinter, J., Herrero-Herranz, E., Weissert, R., Schaeren-Wiemers, N., 2008. Gene expression analysis of normal appearing brain tissue in an animal model for multiple sclerosis revealed grey matter alterations, but only minor white matter changes. J. Neuroimmunol. 205, 10–19.
Zhu, X., Hill, R.A., Dietrich, D., Komitova, M., Suzuki, R., Nishiyama, A., 2011. Age-dependent fate and lineage restriction of single NG2 cells. Development 138, 745–753.